

Effects of friction coefficient and shape of impact object on the fatigue life of specimens with impact damage

Zhan Zhixin^{1,*}, Hu Weiping¹ and Meng Qingchun¹

¹School of Aeronautics Science and Engineering, Beihang University, Beijing, 100191, China

*zzxupc@163.com

Abstract. This paper proposes a new method based on the continuum damage mechanics to analyse the effects of friction coefficient and shape of impact object on the fatigue life, which considers the impact damage, elastic-plastic damage and coupled effects between the stress field and damage field. Firstly, the impact process is simulated and the initial impact damage is calculated. Secondly, the damage-coupled elastic-plastic constitutive equations and fatigue damage evolution equations are used to calculate the fatigue damage of material. Thirdly, the finite element implementation of theoretical models is conducted to conduct fatigue life calculation. At last, effects of friction coefficient and shape of impact object on the fatigue life are discussed.

1. Introduction

In the flight environment, some objects such as birds and metal debris tend to be ingested into the air flow channel and hit on the aircraft turbine engines, which will induce adverse effect on the performance of engine and reduce the fatigue life of structures markedly [1-2]. However, if all of the structures with impact damage are considered to be rejected products, it will be a kind of waste because some defective structures are still enabled to sustain cyclic loading and meet the fatigue life requirements [3]. Thus it's necessary to present a method to evaluate the effect caused by the impact damage and to calculate the fatigue life for structures with impact defect.

Fatigue life prediction for components with impact damage is an important issue in engineering application. In fact, many methods [4-8] such as the stress equivalents, the local stress strain method, the critical plane method and the continuum damage mechanics based method have been proposed to predict the fatigue life of structures. Ferjaoui A et al. [9] used the continuum damage mechanics to conduct the prediction of fretting fatigue crack initiation in double lap bolted joint. Hu P et al. [10] proposed a continuum damage mechanics approach coupled with an improved pit evolution model to predict the fatigue life of the corrosion fatigue of aluminum alloy. Dezecot S et al. [11] conducted the 3D characterization and modeling of low cycle fatigue damage mechanisms at high temperature in a cast aluminum alloy. Mei J et al. [12] presented a comprehensive investigation into non-proportional loading induced multi-axial fatigue damage in aluminum alloys using a recently developed multi-axial fatigue damage parameter. Kumara D et al. [13] conducted the fretting fatigue stress analysis in heterogeneous material using direct numerical simulations in solid mechanics. Bhattia NA et al. [14] used three numerical models to model the effect of both in phase and out of phase loading on contact stresses and damage initiation locations. Pereira K et al. [15] investigated the singularity's presence in fretting fatigue stresses distributions at a contact interface. However, the methods applied to plain fatigue



problems cannot be used directly for failure analyses of defected structures due to the complex effects, such as the impact damage and the redistribution of stress field around the impact pit.

In the previous work [16], the method to calculate the fatigue life for a specimen with an impact pit considering impact damage, residual stress relaxation and elastic-plastic fatigue damage was proposed, but the effects of friction coefficient and shape of impact object on the fatigue life were not discussed. The objective of this study is to research the effects of the two aspects on fatigue life.

2. Theoretical models

2.1. Initial impact damage analysis

In this paper, the quasi-static numerical method is applied to simulate the foreign object impact process. The Armstrong-Frederick elastic-plastic model is used to simulate the constitutive relationship of the structure material.

The deterioration of material induced by the impact can be represented by the damage variable in the framework of continuum damage mechanics. For isotropic materials, the damage variable D [17] is used to represent the stiffness deterioration of RVE (Representative Volume Element), which is expressed by

$$D = \frac{(E - E_D)}{E} \quad (1)$$

where E is Young's Modulus of material and E_D is the effective Young's Modulus of RVE with damage. The size of RVE is about 0.1mm for metals [18]. As E_D ranges from E to 0, D varies between 0 and 1.

After the completion of the residual stress analysis, the initial damage D_0 induced by the plastic deformation can be calculated according to Lemaitre's plasticity damage model [18]:

$$D_0 = \left[\frac{\sigma_{eq}^2 R_v}{2ES} \right]^m \Delta p \quad (2)$$

where σ_{eq} is the equivalent stress and Δp is the accumulated plastic strain. S and m are material parameters. R_v is the triaxiality function.

2.2. Fatigue damage analysis

2.2.1. Damage-coupled elastic-plastic constitutive model

In the frame work of small deformation, total strain ε_{ij} can be divided as

$$\varepsilon_{ij} = \varepsilon_{ij}^e + \varepsilon_{ij}^p \quad (3)$$

where ε_{ij}^e and ε_{ij}^p are elastic strain and plastic strain, respectively. The elastic strain takes the form

$$\varepsilon_{ij}^e = \frac{1+\nu}{E} \left(\frac{\sigma_{ij}}{1-D} \right) - \frac{\nu}{E} \left(\frac{\sigma_{kk} \delta_{ij}}{1-D} \right) \quad (4)$$

where E , ν and σ_{ij} are Young's Modulus, Poisson's ratio and stress components, respectively. The evolution of plastic strain is defined as

$$\dot{\varepsilon}^p = \dot{\lambda} \frac{\partial f}{\partial \sigma_{ij}} = \frac{3}{2} \frac{\dot{\lambda}}{1-D} \frac{S_{ij} \cdot (1-D)^{-1} - \alpha_{ij}}{(S_{ij} \cdot (1-D)^{-1} - \alpha_{ij})_{eq}} \quad (5)$$

$$\dot{p} = \sqrt{\frac{2}{3} \dot{\varepsilon}_{ij}^p \dot{\varepsilon}_{ij}^p} = \frac{\dot{\lambda}}{1-D} \quad (6)$$

where $\dot{\lambda}$ is the plastic multiplier plastic multiplier and S_{ij} is the deviatoric part of the stress, α_{ij} is the deviatoric part of the back stress. The nonlinear kinematic hardening model is used to represent the kinematic hardening behavior

$$\alpha_{ij} = \sum_{k=1}^M \alpha_{ij}^{(k)}, \quad \dot{\alpha}_{ij}^{(k)} = (1-D) \left(\frac{2}{3} C_k \dot{\varepsilon}_{ij}^p - \gamma_k \alpha_{ij}^{(k)} \dot{p} \right) \quad (7)$$

where C_k and γ_k are material constants that can be determined from experimental tests.

2.2.2. Fatigue damage evolution model

Two fatigue damage models are employed to calculate the elastic damage and plastic damage, and the damage evolution rate \dot{D} can be obtained by

$$\dot{D} = \dot{D}_e + \dot{D}_p \quad (8)$$

For the multiaxial cyclic loading, the elastic damage evolution equation [19] of the non-linear continuous damage model can be written as

$$\dot{D}_e = \frac{dD_e}{dN} = [1 - (1 - D)^{\beta+1}]^{\alpha} \cdot \left[\frac{A_{II}}{M_0 (1 - 3b_2 \sigma_{H,m})(1 - D)} \right]^{\beta} \quad (9)$$

where N is the number of cycles until failure, β , M_0 and b_2 are material constants that are determined by fatigue tests. A_{II} is the amplitude of the octahedral shear stress. $\sigma_{H,m}$ is the mean hydrostatic stress.

α is defined: $\alpha = 1 - a \left([A_{II} - \sigma_{I0} (1 - 3b_1 \sigma_{H,m})] / (\sigma_u - \sigma_{e,max}) \right)$, where $\sigma_{e,max}$ is the maximum equivalent stress over a loading cycle. a and b_2 are material constants. The plastic damage evolution equation can be written as

$$\dot{D}_p = \left(\frac{\sigma_{eq}^2 R_v}{2ES(1 - D)^2} \right)^m \dot{p} \quad (10)$$

3. Numerical algorithm and finite element model

3.1. Numerical algorithm

In this study, the damage mechanics finite element numerical method [20-21] is used to calculate the fatigue life of a specimen with impact damage. The entire numerical computation includes simulation of the impact process, calculation of the residual stress, computation of the initial impact damage, and calculation of the elastic-plastic fatigue damage. The detailed steps of the calculation are:

- 1) Initialize all the parameters.
- 2) Conduct a quasi-static simulation analysis of the impact process to obtain the plastic strain field and residual stress field.
- 3) Calculate the initial damage field caused by plastic deformation during the impact process.
- 4) Modify the material properties for each element according to the initial damage. Then the cyclic stress and the accumulated plastic strain are calculated under cyclic loading.
- 5) The increment of fatigue damage can be calculated after ΔN loading cycles, which is given as

$$\Delta D^{(i+1)} = \Delta N \cdot \Delta D_e^{(i+1)} + \Delta N \cdot \Delta D_p^{(i+1)} \quad (11)$$

Then, the total extent of damage corresponding to the total loading cycle of N is obtained as

$$D^{(i+1)} = D^{(i)} + \Delta D^{(i+1)} \quad (12)$$

- 6) If the accumulation of damage at any element reaches 1, a fatigue crack initiates at this element and the corresponding number of cycles is the fatigue crack initiation life, or else, a recalculation of the material properties of each element is conducted using the following equation

$$E^{(i+1)} = E^{(i)} (1 - D^{(i+1)}) \quad (13)$$

Then, the analysis of the stress field and the damage field is repeated until the accumulation of damage at any element reaches 1.

3.2. Finite element model

The material of the specimens in the experiments is TC4 titanium alloy. The method of parameters identification for the above models is presented in the literature [8] and the parameters for TC4 are listed in Table 1. Considering the symmetry of the model, only 1/4 of the model is built and the symmetry boundary conditions are applied at the plane of symmetry. The foreign object is set as rigid and the structure is set as elastoplastic. A 3-D 8-node solid element is used, which is defined by 8 nodes having

three degrees of freedom per node. The mesh density is verified and the convergence analysis of stresses is conducted in order to obtain a converged solution. In total, 54372 elements and 50800 nodes are created. The schematic diagram of model and the established finite element model is shown in figure 1. Cyclic loading is applied in the longitudinal direction with a maximum applied stress of 500 MPa and a stress ratio of 0.1. In the previous research [16], we have validated the CDM approach and we just analyze the effects of friction coefficient and shape of impact object on the fatigue life in this study.

Table 1. The calibrated material parameters.

Elastic damage model	β	M_0	b_1	b_2	a
	1.95	114339	0.001	0.0004	0.72
Plastic damage model	S/MPa		m		
	14429		0.2976		

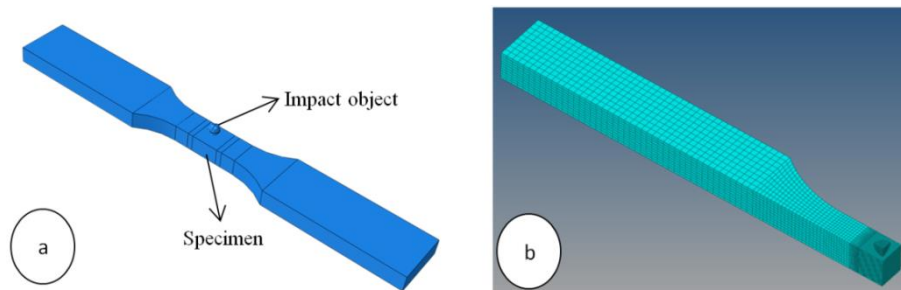


Figure 1. (a) The schematic diagram of whole model; (b) the established finite element model.

4. Computed results and discussions

4.1. Effect of the friction coefficient

The friction coefficient f between the impact object and specimen is an important factor influencing the elastic-plastic damage and fatigue life. The friction coefficient studied here are 0, 0.1 and 0.2, respectively. The radius of impact object is 1.0mm and the depth of impact is 0.43mm.

After conducting the quasi-static simulation of the impact process, the residual stress field can be obtained. The distribution of longitudinal residual stress around the impact pit is shown in figure 2 and the longitudinal residual stress along the distance from the bottom of the impact pit is shown in figure 3. It is clear that the distributions and changing trends of residual stress are similar and the maximum longitudinal compressive residual stress increases with the increase of friction coefficient, which is favourable to increase the fatigue life.

The calculated fatigue lives corresponding to the different friction coefficients are 133175, 181975 and 202475, respectively. It is clear that the fatigue life increases with the increase of friction coefficient. Curves of total damage, initial impact damage, plastic damage and elastic damage versus the number of cycles corresponding to the dangerous element are shown in figure. 4. The changing trend of damage is similar, that is the damage increases slowly in the beginning of loading cycle and faster and faster afterward and the subsequent plastic damage is the dominating compared with the elastic damage.

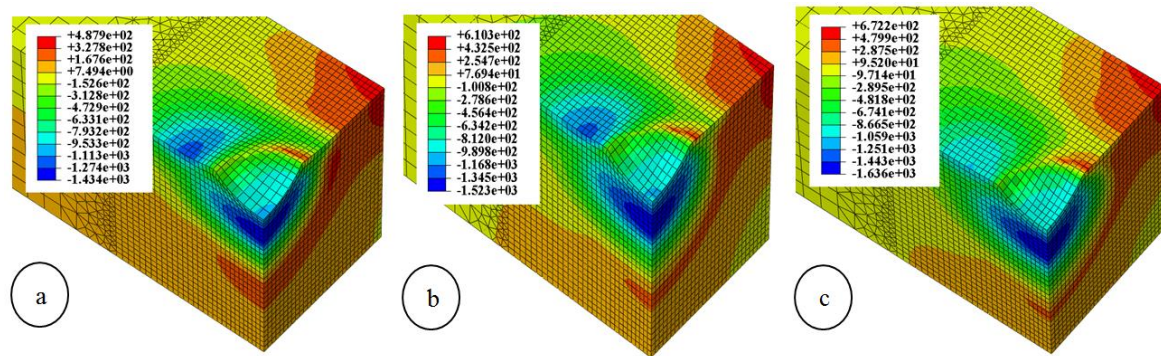


Figure 2. Distribution of longitudinal residual stress with respect to different friction coefficient: (a) $f=0$; (b) $f=0.1$; (c) $f=0.2$.

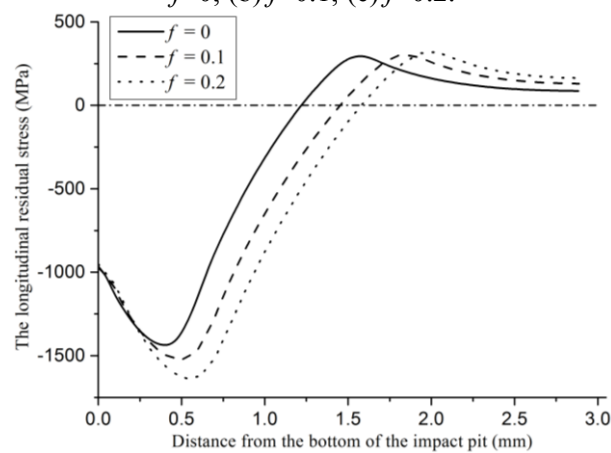


Figure 3. Longitudinal residual stress along the distance from the bottom of the impact pit with respect to different friction coefficient.

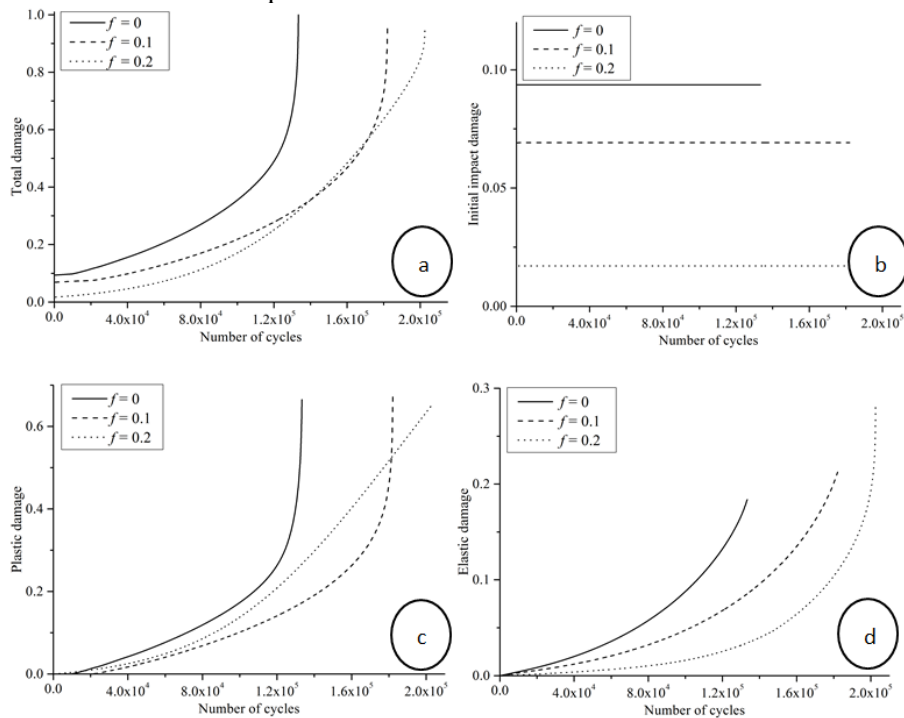


Figure 4. Curves of damage versus the number of cycles with respect to different friction coefficient: (a) total damage, (b) initial impact damage, (c) plastic damage, (d) elastic damage.

4.2. Effect of the shape of impact object

The shape of impact object is another important factor influencing the elastic-plastic damage and fatigue life. The friction coefficient between the impact object and specimen is 0. The depth of impact is 0.43mm. Three different shapes of impact object are discussed. Case 1: spheroid with $a=1$, $b=2$, $c=1$; Case 2: sphere with $R=1$; Case 3: spheroid with $a=2$, $b=1$, $c=1$.

After conducting the quasi-static simulation of the impact process, the residual stress field can be obtained. The distribution of longitudinal residual stress around the impact pit is shown in figure 5 and the longitudinal residual stress along the distance from the bottom of the impact pit is shown in figure 6. It is clear that the maximum longitudinal tensile residual stress of case 1 is much larger than other two cases, which can be adverse to the fatigue life of specimen. We can see that the distributions and changing trends of residual stress along the distance from the bottom of the impact pit with respect to the different shapes of impact object are similar.

The calculated fatigue lives corresponding to the different cases are 119675, 133175 and 163375, respectively. The curves of total damage, initial impact damage, plastic damage and elastic damage versus the number of cycles corresponding to the dangerous element are shown in figure. 7. The changing trend of damage is similar, that is the damage increases slowly in the beginning of loading cycle and faster and faster afterward and the subsequent plastic damage is the dominating compared with the elastic damage.

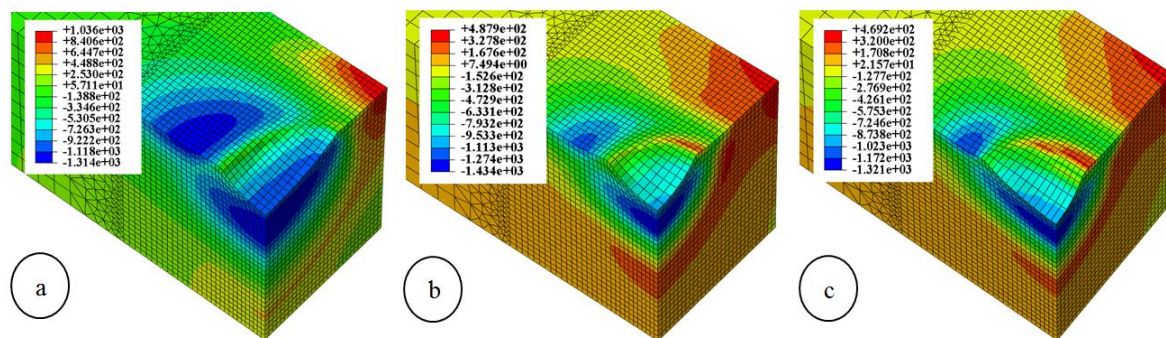


Figure 5. Distribution of longitudinal residual stress with respect to the different shape of impact object: (a) case 1; (b) case 2; (c) case 3.

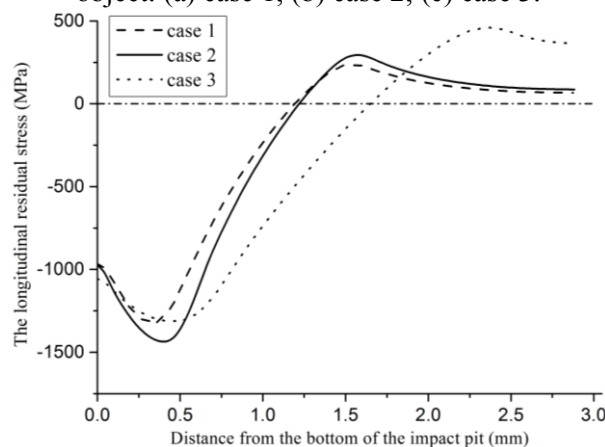


Figure 6. Longitudinal residual stress along the distance from the bottom of the impact pit with respect to the different shape of impact object.

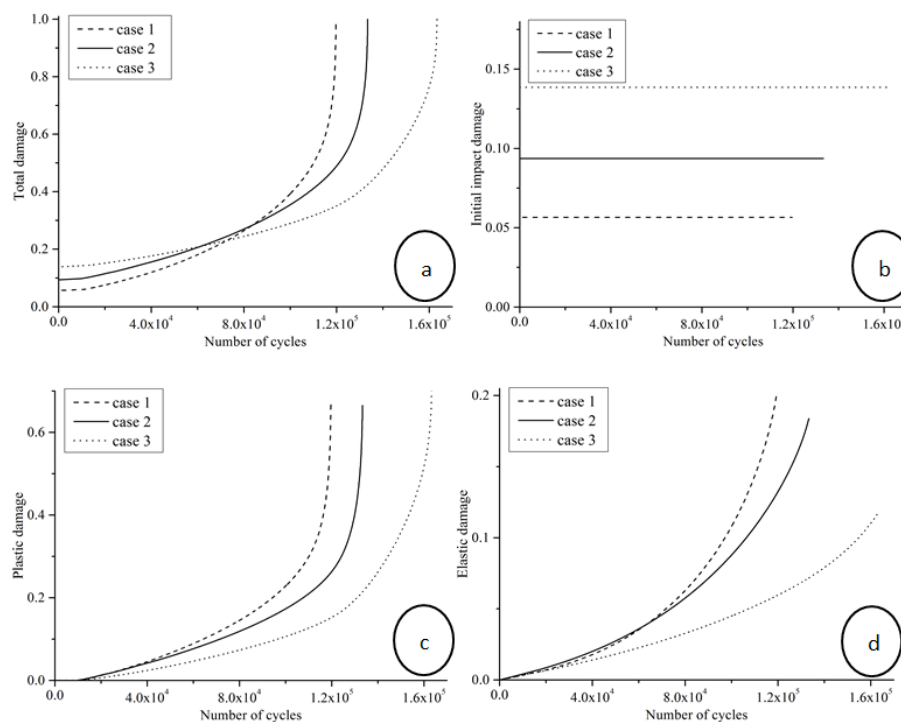


Figure 7. Curves of damage versus the number of cycles with respective to the different shape of impact object: (a) total damage, (b) initial impact damage, (c) plastic damage, (d) elastic damage.

5. Conclusions

In this study, the effects of friction coefficient and shape of impact object on the fatigue life are discussed by using a continuum damage mechanics based method. The following conclusions can be made:

- (1) The impact simulation is conducted and the residual stress and plastic strain fields are obtained, and the initial impact damage is calculated according to the plasticity damage model. Then the fatigue damage evolution equations are used to calculate the fatigue damage of material under cyclic loadings.
- (2) The damage mechanics finite element numerical algorithm is presented which can considers the coupling effect of stress and strain field, initial impact damage and fatigue damage of material.
- (3) Effects of friction coefficient and shape of impact object on the fatigue life are analysed. Firstly, the distributions and changing trends of residual stress are similar for all the cases; secondly, the longitudinal compressive residual stress increases with the increase of friction coefficient, which is favourable for the fatigue life; thirdly, the damage increases slowly in the beginning of loading cycle and faster and faster afterward and the subsequent plastic damage is the dominating compared with the elastic damage for all the cases.

References

- [1] Nowell D, Duo P, Stewart I F. Prediction of fatigue performance in gas turbine blades after foreign object damage. *International journal of fatigue* 2003; 25(9): 963-969.
- [2] Peters J O, Ritchie R O. Influence of foreign-object damage on crack initiation and early crack growth during high-cycle fatigue of Ti-6Al-4V. *Engineering Fracture Mechanics* 2000; 67(3): 193-207.
- [3] Zhan Z, Hu W, Zhang M, et al. Experimental method for and theoretical research on defect tolerance of fixed plate based on damage mechanics. *Chinese Journal of Aeronautics* 2013; 26(5): 1195-1201.
- [4] C.A. Gonçalves, J.A. Araújo, E.N. Mamiya. Multiaxial fatigue: a simple stress based criterion for

- hard metals. *International Journal of Fatigue* 2005; 27(2): 177-187.
- [5] R. Seshadri. The Generalized Local Stress Strain (GLOSS) Analysis—Theory and Applications. *Journal of Pressure Vessel Technology* 1991; 113(2): 219-227.
- [6] Karolczuk A, Macha E. A review of critical plane orientations in multiaxial fatigue failure criteria of metallic materials. *International Journal of Fracture* 2005; 134(3-4): 267-304.
- [7] Chaboche J-L. Continuous damage mechanics—a tool to describe phenomena before crack initiation. *Nuclear Engineering and Design* 1981; 64(2): 233-247.
- [8] Zhan Z, Hu W, Zhang M, et al. Revised damage evolution equation for high cycle fatigue life prediction of aluminum alloy LC4 under uniaxial loading. *Applied Mathematics and Mechanics* 2015; 36(9): 1185-1196.
- [9] Ferjaoui A, Yue T, Wahab M A, et al. Prediction of fretting fatigue crack initiation in double lap bolted joint using Continuum Damage Mechanics. *International Journal of Fatigue* 2015; 73: 66-76.
- [10] Hu P, Meng Q, Hu W, et al. A continuum damage mechanics approach coupled with an improved pit evolution model for the corrosion fatigue of aluminum alloy. *Corrosion Science* 2016; 113: 78-90.
- [11] Dezecot S, Maurel V, Buffiere J Y, et al. 3D characterization and modeling of low cycle fatigue damage mechanisms at high temperature in a cast aluminum alloy. *Acta Materialia* 2017; 123: 24-34.
- [12] Mei J, Dong P. Modeling of path-dependent multi-axial fatigue damage in aluminum alloys. *International Journal of Fatigue* 2017; 95: 252-263.
- [13] Kumar D, Biswas R, Poh L H, et al. Fretting fatigue stress analysis in heterogeneous material using direct numerical simulations in solid mechanics. *Tribology International* 2017; 109: 124-132.
- [14] Bhatti N A, Wahab M A. Finite element analysis of fretting fatigue under out of phase loading conditions. *Tribology International* 2017; 109: 552-562.
- [15] Pereira K, Bordas S, Tomar S, et al. On the Convergence of Stresses in Fretting Fatigue. *Materials* 2016; 9(8): 639.
- [16] Zhan Z, Hu W, Shen F, et al. Fatigue life calculation for a specimen with an impact pit considering impact damage, residual stress relaxation and elastic-plastic fatigue damage. *International Journal of Fatigue* 2017; 96: 208–223.
- [17] Lemaitre J. *Mechanics of solid materials*: Cambridge university press; 1994.
- [18] Lemaitre J, Desmorat R. *Engineering damage mechanics: ductile, creep, fatigue and brittle failures*: Springer; 2005.
- [19] Marmi A K, Habraken A M, Duchene L. Multiaxial fatigue damage modelling at macro scale of Ti–6Al–4V alloy. *International Journal of Fatigue* 2009; 31(11): 2031-2040.
- [20] Zhan Z, Hu W, Zhang M, et al. The fatigue life prediction for structure with surface scratch considering cutting residual stress, initial plasticity damage and fatigue damage. *International Journal of Fatigue* 2015; 74: 173-182.
- [21] Zhan Z, Hu W, Meng Q, et al. Continuum damage mechanics-based approach to the fatigue life prediction for 7050-T7451 aluminum alloy with impact pit. *International Journal of Damage Mechanics* 2016; 25(7): 943-966.